ELSEVIER

Clinical Neurophysiology xx (2004) 1–9

www.elsevier.com/locate/clinph

Slow-wave activity arising from the same area as epileptiform activity in the EEG of paediatric patients with focal epilepsy

Bart Vanrumste[a,b,c,*], Richard D. Jones[a,c,d], Philip J. Bones[a], Grant J. Carroll[e]

[a]*Department of Electrical and Computer Engineering, University of Canterbury, Private Bag 4800, Christchurch, New Zealand*
[b]*Department of Electrical Engineering (ESAT/SCD), Katholieke Universiteit Leuven, Kasteelpark Arenberg 10, B-3001 Leuven, Belgium*
[c]*Department of Medical Physics and Bioengineering, Christchurch Hospital, Private Bag 4710, Christchurch, New Zealand*
[d]*Department of Medicine, Christchurch School of Medicine and Health Science, P.O. Box 4345, Christchurch, New Zealand*
[e]*Department of Neurology, Christchurch Hospital, Private Bag 4710, Christchurch, New Zealand*

Accepted 31 July 2004

Abstract

Objective: The aim of this study was to investigate the presence and characteristics of apparent non-epileptiform activity arising in the same brain area as epileptiform activity in the EEG of paediatric patients with focal epilepsy.

Methods: The EEG from eight patients was analysed by an automated method which detects epochs with a single underlying source having a dipolar potential distribution. The EEG with the highlighted detections was then rated by a clinical neurophysiologist (EEGer) with respect to epileptiform activity.

Results: Although EEGer-marked events and computer detections often coincided, in five out of the eight patients, a substantial number of other detections were found to arise from the same area as the marked events. The morphology of a high proportion of these other detections did not resemble typical epileptiform activity and had a frequency content mainly in the delta and theta ranges.

Conclusions: This is, to our knowledge, the first study to use an automated technique to demonstrate the presence of non-epileptiform activity arising from the same area as the epileptiform activity in the EEG of paediatric patients with focal epilepsy. This slow wave activity is likely to be related to the underlying epileptogenic process.

Significance: This paper suggests a technique for automated detection of focal activity arising from epileptogenic foci. It also provides a new perspective on extracting clinical useful information from slow-wave background EEG activity.
© 2004 International Federation of Clinical Neurophysiology. Published by Elsevier Ireland Ltd. All rights reserved.

Keywords: Paediatric patients; Focal epilepsy; EEG dipole modelling; Singular value decomposition; Epileptiform activity; Unidentified focal events

1. Introduction

The background EEG in patients with focal epilepsy often shows focal or localised delta activity (<4 Hz) related to the disorder (Panet-Raymond and Gotman, 1990). Intermittent delta activity in the EEG of patients with focal epileptogenic brain lesions has been reported to be a marker for the existence of an epileptogenic focus (Gambardella et al., 1995). Similarly, Huppertz et al. (2001) used dipole localization to show delta activity coming from cortical regions close to the brain lesion. Gallen et al. (1997) selected epochs showing abnormal low-frequency activity in the magnetoencephalogram (MEG). The underlying equivalent current dipole of this activity was found to be useful in the presurgical evaluation of patients with epilepsy.

In the above studies, the epochs were visually selected by an EEGer and related to abnormal activity in the delta range. In a group of patients with cerebral tumors de Jongh et al. (2001) automatically examined the MEG for dipolar activity. They found that dipoles describing delta and theta activity were located ipsilateral to lesions.

Preliminary observations from our own comparisons of transient events detected by computer algorithm with those of an EEGer have led us to the study reported here.

* Corresponding author. Tel.: +32 16 321884; fax: +32 16 321970.
E-mail address: bart.vanrumste@esat.kuleuven.ac.be (B. Vanrumste).

1388-2457/$30.00 © 2004 International Federation of Clinical Neurophysiology. Published by Elsevier Ireland Ltd. All rights reserved.
doi:10.1016/j.clinph.2004.07.032

We applied a method that automatically detected dominant events with a dipolar scalp potential distribution in 19-channel EEG of paediatric patients with focal epilepsy. In addition, the algorithm provided the dipole location (within a spherical 3-shell model) associated with each detection. The EEGer was asked to identify all epileptiform events after being given the EEG recording with all computer detections already high-lighted. A region of interest (ROI) was than identified based on the computer-detected epileptiform-events. Finally, as a second part of this study, computer-detected non-epileptiform-events with dipoles in the ROI were further categorized by the EEGer with respect to the traditional frequency bands.

2. Patients and EEG

Nineteen-channel EEGs (10–20 international electrode placement, 1–30 Hz band-pass filtered, sampled at 256 Hz, common referenced) of eight paediatric patients with focal epilepsy were recorded. The patients had been selected out of a pool of available data. The EEG recordings ranged from 12.4 to 21.2 min. The patients had an average age of 5.5 years (range 3–10 years). The EEG and brain scan (MRI, CT) findings for each patient are summarized in Table 1.

3. Methods

The method comprised of applying a computer detection algorithm to the 19-channel EEG, having the EEGer categorize the EEG within which computer detections were highlighted, and constructing a ROI based on the dipoles of epileptiform-events computer-detected.

3.1. Detection method

The detection algorithm was based on a novel method developed for detection of epileptiform activity in multi-channel EEG recordings (Van Hoey, 2000; Vanrumste et al., 2002). Fig. 1 shows a flowchart of the method. The 19-channel EEG was first transformed from common referencing to average referencing. It was then divided into overlapping epochs of 250 ms (64 samples). Each epoch was shifted in time from the previous one by 31.25 ms (eight samples). The epochs were processed in two steps. The first step involved singular value decomposition (SVD) (Datta, 1995) to inspect the number of generators active in the epoch. The EEG epoch $\mathbf{V} \in \mathbb{R}^{19\times 64}$ was decomposed by SVD into $\mathbf{U}\cdot\mathbf{s}\cdot\mathbf{W}^T$ (T, transpose operator) with 19 'potential distributions' found in the columns of $\mathbf{U} \in \mathbb{R}^{19\times 19}$, 19 corresponding time courses in the columns of $\mathbf{W} \in \mathbb{R}^{64\times 19}$ and the singular values s_i found on the diagonal entries of diagonal matrix $\mathbf{s} \in \mathbb{R}^{19\times 19}$. The s_i values, representing the square-root of the energy contribution of component i, were ordered such that the one with the largest value had the smallest index i. SVD was used to inspect the number of generators active in the epoch. A detection was said to have occurred when only one generator was predominantly active in the epoch. The measure

$$S = \frac{s_1^2}{\sum_{i=1}^{19} s_i^2}, \tag{1}$$

was used for this purpose, where S is the fraction of energy contained in the first component. If S was higher than 70%, a dominant generator was assumed.

In the second step, EEG dipole source analysis was applied to the potential distribution $\mathbf{U}_{*1}$ (the left eigenvector corresponding to the first singular value) of the dominant generator. A three-shell spherical head model was used with the radii for the brain, skull and scalp compartment being 80, 85 and 92 mm, respectively (Rush and Driscoll, 1968). The relative conductivities with respect to the skull conductivity of the three compartments were 16, 1 and 16, respectively (Oostendorp et al., 2000). The optimum dipole was found by changing the dipole parameters until a minimum was found in the cost-function given by the relative

Table 1
Summary of EEG and medical imaging findings for the eight patients

Patient	Sex/age	EEG summary	Brain scan summary
1	F/3	Diffuse excess of fast activity and frequent discharges in left occipital region	Diffuse hypoxic/ischaemic brain injury (CT)
2	F/4	Discharges predominantly from right parietal region, plus slower background from this region	No record
3	F/5	Right central and midtemporal discharges	Destructive white matter lesion in right frontal lobe (MRI)
4	M/5	Occipital sharp waves typical of benign occipital epilepsy	Normal (MRI)
5	M/6	Drug induced beta, right antero-temporal to midtemporal sharp wave discharges	No record
6	M/7	Right Centro-temporal sharp wave discharges	Normal (CT)
7	M/4	Parasagittal epileptiform discharges prominent from the left central region	Moderately extensive left-sided infarction (MRI)
8	F/10	Slowing in right anterior quadrant and epileptiform discharges	Right frontal lobe lesion (MRI)

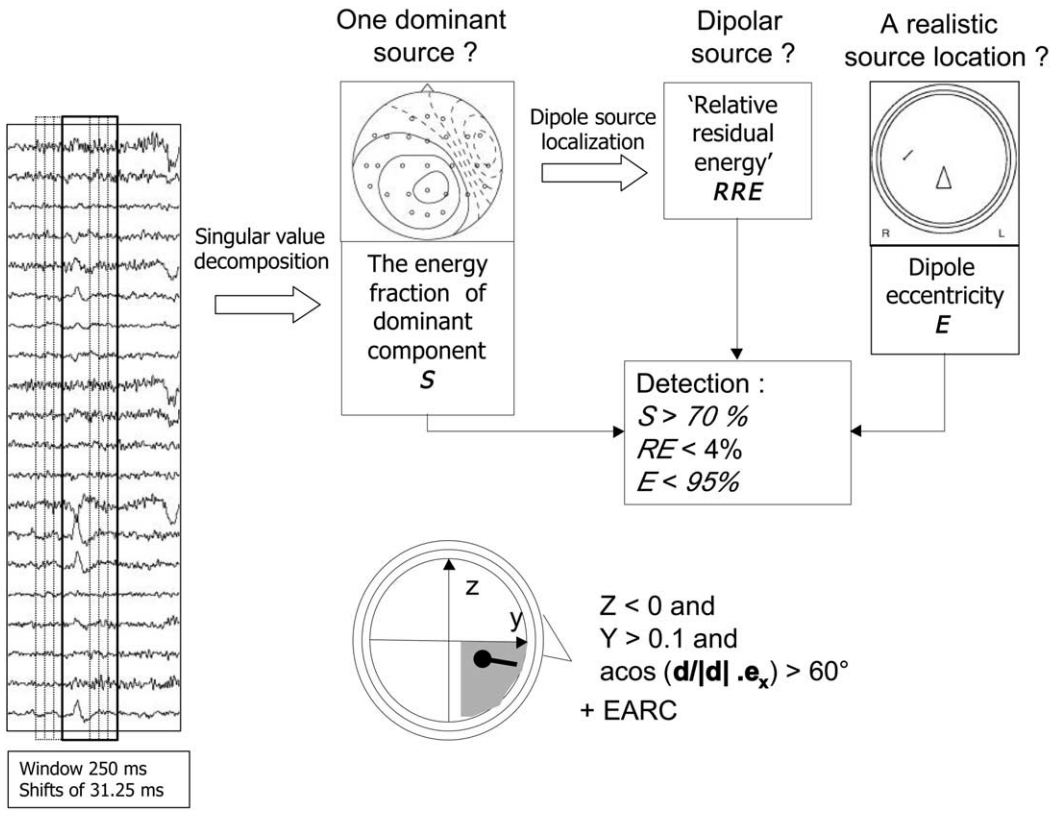

Fig. 1. A flowchart of the method for detecting focal sources in the EEG.

residual energy (RRE),

$$\mathrm{RRE} = \frac{\|\mathbf{U}_{*1} - \mathbf{V}_{\mathrm{model}}\|^2}{\|\mathbf{U}_{*1}\|^2}, \tag{2}$$

with $\mathbf{V}_{\mathrm{model}}$ being the potentials generated by the fitted dipole in the three shell spherical model. The RRE gives the fraction of energy, which cannot be explained by a dipolar field. The smaller the RRE the better the dominant potentials obtained from the SVD represent a dipolar source and, hence, a focal source. Dipolar field distributions can also be generated by more extended sources (Hara et al., 1999) but the spatial extent of these sources is difficult to estimate. The detection algorithm triggered an EEG epoch when SVD indicated a dominant source and the RRE was lower than 4%.

Certain artifacts were subsequently removed by applying rejection rules based on the dipole model in the three-shell spherical head model (Flanagan et al., 2003). First, the relative eccentricity (ECC) of the dipole position was calculated with respect to the radius of the inner shell. If the ECC was found to exceed 95%, the dipole was rejected on the grounds of being either an eye-blink or an electrode artifact. A further eye-blink artifact removal criterion (EARC) was introduced to reject epochs from a dipole located in the lower frontal area. A dipole with position $\mathbf{r}[r_x\ r_y\ r_z]$, normalized to the radius of the outer shell, (x-axis: left to right ear, y-axis: anterior to posterior, z-axis: vertical through Cz and origin in the center of the spheres) and orientation $\mathbf{d}[d_x\ d_y\ d_z]$ was removed when $(r_z < 0) \wedge (r_y > 0.1) \wedge (\arccos(\mathbf{d}/\|\mathbf{d}\|) \cdot \mathrm{e}_x)) > 60°)$ was true, with $\|\ \|$ the euclidian norm, $\cdot$ the inner product, $\wedge$ the AND operator and $\mathbf{e}_x$, the unity vector along the x-axis; that is, the detection was rejected if the computed dipole was located in the lower frontal area and its dipole moment vector made an angle of a least 60° with the x-axis.

In summary, an epoch was detected when four conditions were fulfilled: $S > 70\%$ indicating a dominant generator in the epoch, $\mathrm{RRE} < 4\%$ demonstrating that a dipole was a good model for that generator, $\mathrm{ECC} < 95\%$ indicating removal of electrode or eye-blink artifacts and the EARC not being met, suggesting that the epoch was not due to an eye-blink artifact. Importantly, this method detects focal activity regardless of the morphology of the activity and the amount of total power in the epoch.

As the EEG is segmented into overlapping epochs, it is possible for a single event to be detected more than once. Detected epochs were therefore clustered into a *detection.* Two consecutive detected epochs were clustered if they both started within 250 ms of each other and had their associated dipole positions $\mathbf{r}_1$ and $\mathbf{r}_2$ located in the same region (i.e. $\|r_1 - r_2\| < 0.2$ or 18.4 mm.). This was done to prevent activity in different brain regions being clustered as one detection. The dipole parameters associated with the detection were then obtained by averaging the dipole parameters associated with the detected epochs within it.

The thresholds for *S*, RRE and ECC were chosen as follows. The EEG of patient 7 was marked for epileptiform events by the EEGer before being remarked with the automatic detections highlighted. For a given set of thresholds of these properties, a sensitivity (#detections also marked by the EEGer/#EEGer marked events) and selectivity (#detections also marked by the EEGer/#detections) to epileptiform events was obtained. The selectivity was then plotted versus sensitivity for a large number of threshold sets. The envelope curve, also called the receiver operator characteristic (ROC) curve, represented the best possible combinations of sensitivity and selectivity. The thresholds mentioned above were associated with a position on the ROC with a sensitivity and selectivity of 78 and 13%, respectively, in patient 7. The same thresholds were used for the other patients. The parameters associated with the EARC were kept fixed in this preprocessing step.

3.2. Categorising the EEG

The EEGs with the detections highlighted were then presented to the EEGer who was asked to indicate all events which he considered to be definitely epileptiform or questionably epileptiform. Epileptiform patterns were defined as per Chatrian et al. (1974) as: 'Applies to distinctive waves or complexes, distinguished from background activity, and resembling those recorded in proportion of human subjects suffering from epileptic disorders and in animals rendered epileptic experimentally. Epileptiform patterns include spikes and sharp wave, alone or accompanied by slow waves, occurring singly or in bursts lasting at most a few seconds'. (In what follows we use 'epileptiform events' and 'epileptiform activity' as synonyms of 'epileptiform patterns'.) Detections not marked by the EEGer were, in his opinion, Non-Epileptiform-patterns computer-Detected (NEDs).

Definite and questionable epileptiform events (marked by the EEGer), which coincided with computer detections were termed Definite-Epileptiform-patterns computer-Detected (DEDs) and Questionable-Epileptiform-patterns computer-Detected (QEDs) respectively.

3.3. Construction of a region of interest

To further process the NEDs, a spherical ROI was established to indicate the origin of the epileptiform patterns. Ideally, one would construct this region based only on DEDs as they are, in the EEGers' opinion, unequivocally epileptiform. However, when the number of DEDs is too small (two or less), QEDs were also utilized to construct the ROI; this was the case in four of the eight EEGs (see Table 2). The centre of the region was obtained by averaging the dipole positions of the DEDs or, DEDs and QEDs. The maximum of the standard deviations from that average along the cartesian axes (i.e. $\max(\sigma_x, \sigma_y, \sigma_z)$) ranged from 0.08 to 0.23 relative to the outer radius of the head model in the eight patients. A radius of 0.2 (i.e. 18.4 mm) was then chosen to establish a volume around the centre of the sphere. NEDs located in that spherical ROI were termed Non-Epileptiform-patterns computer-Detected In Region of interest (NEDIRs).

Table 2
Computer detections categorized by EEGer into definite, questionable or non epileptiform patterns

Patient	DEDs	QEDs	NEDs	NEDIRs
1	24 (65) ✓	21 (97)	93	30 (32%)
2	0 (6)	32 (92) ✓	83	30 (36%)
3	1 (1) ✓	87 (105) ✓	243	120 (49%)
4	27 (96) ✓	22 (88)	89	1 (1.1%)
5	1 (16) ✓	2 (159) ✓	5	0 (0%)
6	1 (7) ✓	11 (31) ✓	100	3 (3%)
7	17 (19) ✓	40 (66)	47	21 (44.6%)
8	22 (102) ✓	84 (167)	595	105 (17.6%)

DEDs is number of definite-epileptiform-patterns computer-detected. QEDs is number of questionable-epileptiform-patterns computer-detected. Figures in parentheses give the total number of definite/questionable epileptiform patterns marked by the EEGer. Detections used to determine the centre of the region of interest are marked with '✓'. (NEDs is number of non-epileptiform-patterns computer-detected. (NEDIRs is number of NEDs located in the region of interest; the values in parentheses give the percentage of NEDs which are NEDIRs.

4. Results

Table 2 shows the computer detections in each EEG divided into definite, questionable and non-epileptiform patterns according to the EEGer. The total number of definite or questionable epileptiform events marked by the EEGer are also shown. Note that in patients other than 7, the number of DEDs and QEDs are only a small subset of the definite and questionable epileptiform events marked by the EEGer, indicating that the method with the thresholds (fine-tuned for patient 7) fixed over the entire patient group performed sub-optimally as a spike detector. Nevertheless, for our purposes, this number was sufficient to obtain a reasonable estimate of the epileptogenic region.

For patient 2, no DEDs were available. Hence, for this patient the QEDs were used to define the ROI from where the epileptiform activity originates. As the numbers of DEDs were too small for patient 3, 5 and 6, both the DEDs and QEDs were used to define the ROI.

The numbers of NEDIRs are also given in Table 2. For a uniform distribution of NEDs, the proportion of NEDIRs (given in parenthesis) would be 1.22% $((0.2/(80/92))^3 100)$ For patients 4, 5 and 6 the proportion is of this order indicating that there was no strong association between NEDs and the epileptiform activity in these three patients. Conversely, for the remaining five patients this percentage was substantially higher, indicating a close-proximity link between the NEDs and the epileptiform activity.

The dipoles of DEDs for all patients are shown in Fig. 2(a). A frontal-, top- and side-view of the same group of dipoles is illustrated to give a better understanding of the 3D position of the dipoles in the head model. The dipoles of the QEDs are given in Fig. 2(b). These dipoles are clustered in brain regions, which correspond with the areas in which the EEGer detected epileptiform events as given in Table 1. Note that most dipole orientations tend to be in the same direction.

Fig. 2(c) shows dipole positions of the NEDs. The dipole orientations have been omitted to make the plots easier to read. The ROI encapsulating the NEDIRs is also shown.

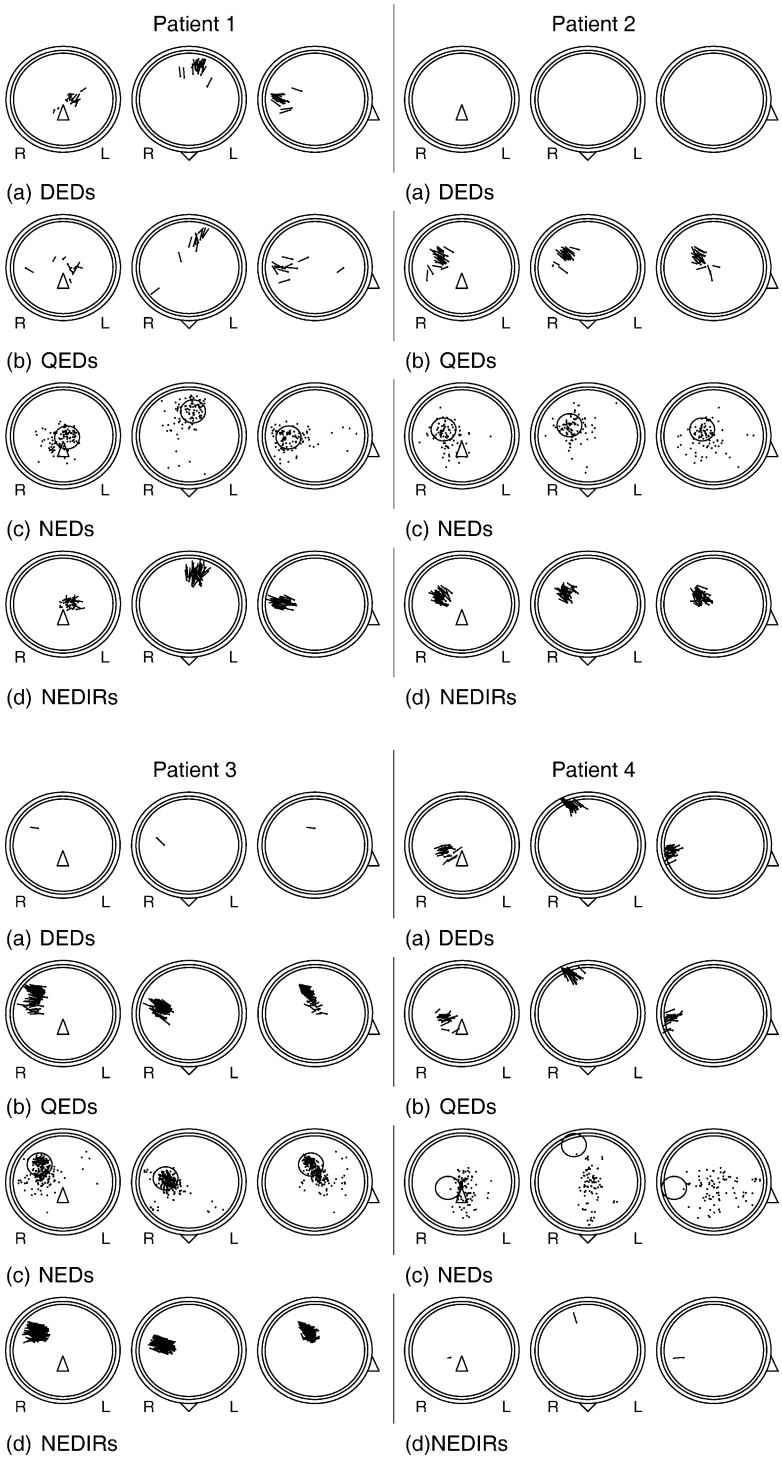

Fig. 2. Dipoles of DEDs (a) and QEDs (b) for all patients. The dipoles are shown in frontal-, top- and side view, respectively. Dipoles associated with NEDs are shown in (c); the ROI which encapsulates NEDIRs is also shown but not the dipole orientation. The dipoles of the NEDIRs are shown in (d).

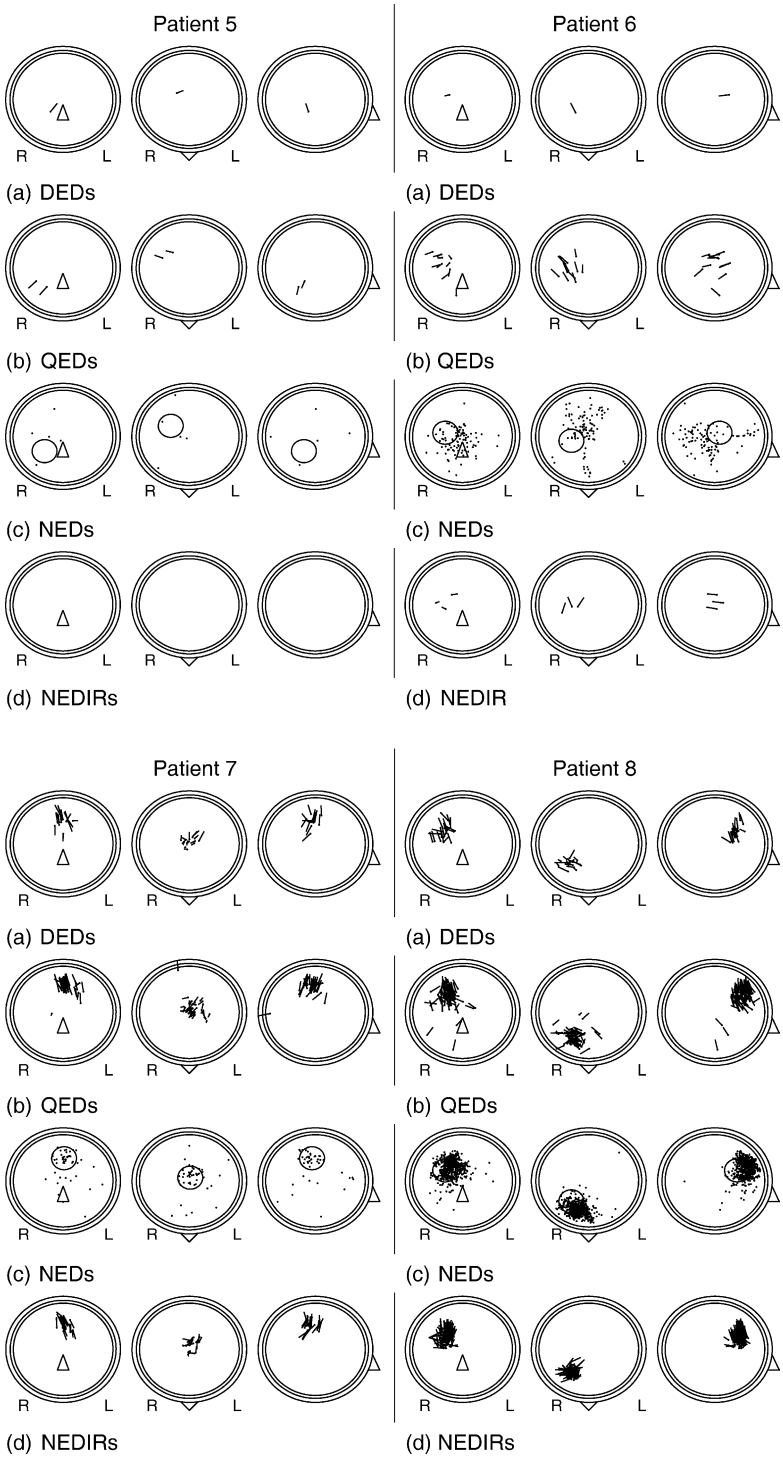

Fig. 2 (*continued*)

For patients 1–3, 7 and 8, a large number of dipoles are located in the same area (both within and immediately outside the ROI) as the dipoles associated with the detections marked by the EEGer. Hence, it is clear that the dipoles of the NEDs are not randomly distributed in the spherical head model and their strong predominance in the same region as the detected epileptiform events has not occurred by chance. For patients 4 and 6 a large number of dipoles did not cluster in the region where the epileptiform activity originates. Looking at the EEG of all NEDs, alpha activity and eyeblink artifacts were associated with these detections in these patients. For patient 5 only a small number of NEDs was observed due to the small number of detections obtained by the algorithm.

Finally, Fig. 2(d) shows the dipole positions of the NEDIRs. It is striking that these orientations are very similar to those of the dipoles for the DEDs and QEDs.

5. Further analysis

In the second part of the study the EEGer was asked to re-examine the EEG, centred on 5 s epochs, of all NEDIRs and to exclude any possible epileptiform activity or artifacts. The numbers of possible Epileptiform events or Artifacts (e./a.) in the NEDIRs are given in column '(e./a.' in Table 3. For patients 1–3 and 8 this represents a substantial subset of the NEDIRs. This process upgraded NEDIRs to QEDs and removed artifacts from the NEDIRs.

The remaining NEDIRs were termed unidentified focal events (UFEs). The EEGer classified these UFEs into the traditional EEG frequency bands (i.e., delta (<4 Hz), theta (4–8 Hz), alpha (8–13 Hz) and beta (>13 Hz)). The numbers of UFEs in each of these groups are given in columns marked '#δ', '#θ', '#α' and '#β' in Table 3. The dominant frequency of the majority of UFEs was in the delta and theta ranges.

The EEG of representative UFEs is shown in Fig. 3. The 5 s EEG is centred around the UFE, which is bounded by vertical dotted lines. These lines indicate the start and end of the computer detection, which can consist of several detection epochs. The vertical dash-dotted lines are events (questionable or definite) marked by the EEGer. Below the EEG, the temporal vector of the first (most dominant) component of the SVD is given for each epoch in the detection. Fig. 3 shows examples of UFEs categorized as predominantly delta ((a) and (b)) or theta ((c) and (d)).

6. Discussion

For five of the eight patients (patients 1–3, 7 and 8) the NEDs were clearly from the same region as DEDs and QEDs, as indicated in Fig. 2(c). Furthermore, the morphology of UFEs contained no epileptiform patterns as defined by (Chatrian et al., 1974). Similar to the findings of de Jongh et al. (2001) with the brain tumour patients, the spectral content of most of the UFEs for these paediatric patients was mainly in the delta and theta ranges, in contrast to only slow delta activity as reported in other studies (Gallen et al., 1997; Gambardella et al., 1995; Panet-Raymond and Gotman, 1990; Gibbs et al., 1993). In the latter studies the events were visually selected while in our case and that of de Jongh et al. they were detected by an automated technique.

In patient 1, a diffuse non-focal brain lesion was observed on CT (Table 1) suggesting that UFEs can occur in patients with focal epilepsy other than the presence of focal brain lesions as previously reported. However, this result is still speculative and a larger sample is required to confirm this finding. It is also possible that UFEs may result from a brain lesion irrespective of any associated epileptogensis. To address these two possibilities a larger sample is required.

In patients 4 and 6, the NED were found to be more spread out, as shown in Fig. 2(c), with no strong cluster in the same area as the DEDs and QEDs. This indicates that the detection method has by chance detected NEDs in the DED/QED zone, which are probably not related to the underlying epilepsy. In patient 5, only eight computer detections were found. Drug-induced beta activity (Duncan, 1987) was superimposed on the background EEG leaving the *S* measure below the threshold of 70%. No single dominant source could be observed.

The NED clusters for patients 1–3, 7 and 8 are in quite different brain regions (Fig. 2(c)), indicating that the detection algorithm has no obvious bias regarding preferential brain region.

Importantly, the method is not sensitive to the waveform of the events, in contrast to mimetic detection methods (Gotman and Gloor, 1976; Dingle et al., 1993). This would be a disadvantage if the algorithm was used to detect epileptiform patterns, but is an advantage in the current study as it enables focal events to be detected, independent of morphology. The *S* measure looks at relative energy levels and, hence, the method can still work with relatively low absolute energy levels, in contrast to the method used

Table 3
Re-examination of NEDIRs by EEGer

Patient	#NEDIRs	#e./a.	#UFEs	#δ	#θ	#α	#β
1	30	13	17	10	7	–	–
2	30	25	5	2	3	–	–
3	120	72	48	9	36	3	–
4	1	–	1	–	1	–	–
5	0	–	–	–	–	–	–
6	3	–	3	1	1	–	1
7	21	–	21	9	11	–	1
8	105	21	84	36	42	6	–

#NEDIRs is number of NEDs located in the region of interest. #e./a. is numbers of NEDIRs upgraded to questionable epileptiform patterns or possible artifacts by EEGer on re-examination. #UFEs is numbers of the rest of the NEDIRs. '#δ', '#θ', '#α' and '#β' are numbers of UFEs, which were considered to have prominent delta-activity (<4 Hz), theta-activity (4–8 Hz), alpha-activity (8–13 Hz) and beta-activity (>13 Hz), respectively.

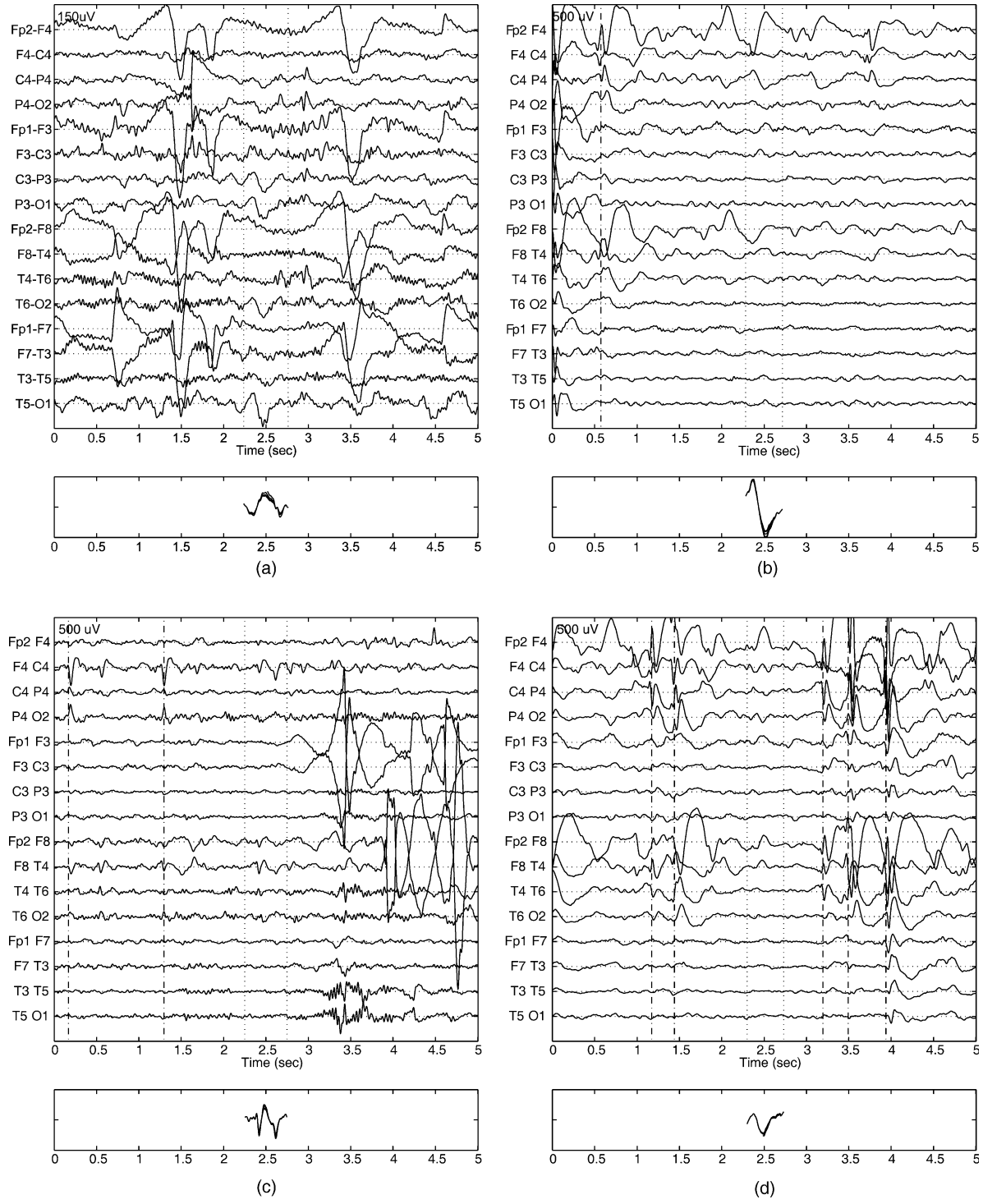

Fig. 3. The EEG is shown of UFEs with predominant delta (<4 Hz) activity in (a) (patient 1) and (b) (patient 8), and with mainly theta activity (4–8 Hz) in (c) (patient 3) and (d) (patient 8). The EEG between the dotted lines represents the detection. The temporal vector of the first SVD component for each epoch in the detection is given below the EEG. The dot-dashed lines represent EEGer-marked event.

by de Munck et al. (2001), which uses thresholds based on the absolute energy levels.

To automate the grouping of the detections, clustering algorithms based on the dipole coordinates, reported by Ossadtchi et al. (2004) and, on the potential distribution, reported by Van 't Ent et al. (2003), could also be applied in the future.

Although we have demonstrated a dominant presence of non-epileptiform patterns in the EEG from the same region as the epileptiform focus in the majority of a group of

paediatric patients with focal epilepsy, their origin and morphology need to be confirmed by depth-electrodes as was done in a study by Lopes da Silva et al. (1977). Depth-electrode studies would also allow investigations of the role which UFEs have in the epileptogenic process.

It would also be of interest to undertake further studies to determine whether the presence and characteristics of the UFEs in focal epilepsy are any different in adult patients.

Finally, EEG recordings between seizures may contain no epileptiform patterns in approximately 20–40% of patients with a history of seizures (Fisch, 1999). By applying our approach it may be possible to demonstrate focal interictal 'non-epileptiform' activity in the EEG of these patients which correlates with their clinical history of seizures.

Acknowledgements

Bart Vanrumste was a Postdoctoral Fellow funded by the University of Canterbury, Christchurch, New Zealand, until November 2003. Since then he is postdoctoral fellow at K.U. Leuven in Belgium and funded by the 'Programmatorische Federale Overheidsdienst Wetenschapsbeleid' of the Belgian Government.

References

Chatrian GE, Bergamini L, Klass DW, Lennox-Buchthall M, Petersén I. A glossary of terms most commonly used by clinical electroencephalographers. Electroencephalogr Clin Neurophysiol 1974;37:538–48.

Datta BN. Numerical linear algebra and applications. Brooks: Cole Publishing Company; 1995.

de Jongh A, Munck JCD, Baayen JC, Jonkman EJ, Heethaar RH, Dijk BWV. The localization of spontaneous brain activity: first results in patients with cerebral tumors. Clin Neurophysiol 2001;112(2):378–85.

de Munck JC, de Jongh A, Van Dijk BW. The localization of spontaneous brain activity: an efficient way to analyze large data sets. IEEE Trans Biomed Eng 2001;48(11):1221–8.

Dingle AA, Jones RD, Carroll GJ, Fright WR. A multi-stage system to detect epileptiform activity in the EEG. IEEE Trans Biomed Eng 1993;40:1260–8.

Duncan J. Antiepileptic drugs and the electroencephalogram. Epilepsia 1987;28:259–66.

Fisch BJ. Fisch and Spehlmann's EEG Primer: basic principles of digital and analog EEG. Amsterdam: Elsevier; 1999.

Flanagan D, Agarwal R, Wang Y, Gotman J. Improvement in the performance of automated spike detection using dipole source features for artefact rejection. Clin Neurophysiol 2003;114(1):38–49.

Gallen CC, Tecoma E, Iragui V, Sobel DF, Schwartz BJ, Bloom FE. Magnetic source imaging of abnormal low-frequency magnetic activity in presurgical evaluations of epilepsy. Epilepsia 1997;38(4):452–60.

Gambardella A, Gotman J, Cendes F, Andermann F. Focal intermittent delta activity in patients with mesiotemporal atrophy: a reliable marker of the epileptogenic focus. Epilepsia 1995;36(2):122–9.

Gibbs J, Appleton R, Carty H, et al. Focal electroencephalographic abnormalities and computerised tomography findings in children with seizures. J Neurol Neurosurg Psychiatry 1993;56:369–71.

Gotman J, Gloor P. Automatic recognition and quantification of interictal epileptic activity in the human scalp EEG. Electroencephalogr Clin Neurophysiol 1976;41:513–29.

Hara J, Musha T, Shankle WR. Approximating dipoles from human EEG activity: the effect of dipole source configuration on dipolarity using single dipole models. IEEE Trans Biomed Eng 1999;46(2):125–9.

Huppertz HJ, Hof E, Klisch J, Wagner M, Lucking CH, KristevaFeige R. Localization of interictal delta and epileptiform EEG activity associated with focal epileptogenic brain lesions. Neuroimage 2001;13(1):15–28.

Lopes da Silva FH, Van Hulten K, Lommen JG, Storm Van Leeuwen W, Van Veelen CWM, Vliegenthart W. Automatic detection and localization of epileptic foci. Electroencephalogr Clin Neurophysiol 1977;43(1):1–13.

Oostendorp TF, Delbeke J, Stegeman DF. The conductivity of the human skull: Results of in vivo and in vitro measurements. IEEE Trans Biomed Eng 2000;47(11):1487–92.

Ossadtchi A, Baillet S, Mosher JC, Sutherling W, Leahy RM. Automated interictal spike detection and source localization in magnetoencephalography using independent components analysis and spatio-temporal clustering. Clin Neurophysiol 2004;115:508–22.

Panet-Raymond D, Gotman J. Asymmetry in delta activity in patients with focal epilepsy. Electroencephalogr Clin Neurophysiol 1990;75:474–81.

Rush S, Driscoll DA. Current distribution in the brain from surface electrodes. Anesth Analg 1968;47:717–23.

Van Hoey G, Detectie en bronlokalisatie van epileptische hersenactiviteit met behulp van EEG-signalen. PhD thesis, Ghent University, Belgium, in Dutch, 2000.

Van 't Ent D, Manshanden I, Ossenblok P, Velis DN, de Munck JC, Verbunt JPA, Lopes da Silva FH. Spike cluster analysis in neocortical localization related epilepsy yields clinically significant equivalent source localization results in meg. Clin Neurophysiol 2003;114(10):1948–62.

Vanrumste B, Jones RD, Bones PJ. Detection of focal epileptiform activity in the EEG: an SVD and dipole model approach. In: Proceedings of the second joint EMBS/BMES conference. vol. 3. Houston, TX, USA; 2002, p. 2031–2.